

R

REFERENCE

AAE



AAEC/E435

AUSTRALIAN ATOMIC ENERGY COMMISSION
RESEARCH ESTABLISHMENT
LUCAS HEIGHTS

AN ANALYSIS OF SELF-TERMINATING POWER
TRANSIENTS IN THE REACTOR HIFAR

by

J.W. CONNOLLY
H. FERGUSON

February 1978

ISBN 0 642 59644 1

AUSTRALIAN ATOMIC ENERGY COMMISSION

RESEARCH ESTABLISHMENT

LUCAS HEIGHTS

AN ANALYSIS OF SELF-TERMINATING POWER

TRANSIENTS IN THE REACTOR HIFAR

by

J. W. CONNOLLY

H. FERGUSON

ABSTRACT

The consequences of step reactivity additions above critical have been calculated for HIFAR under conditions of no coolant flow and the operating coolant flow rate of 400 kg s^{-1} . In particular, the maximum core excess reactivity that will allow loss of a central coarse control arm blade from the core has been determined.

In order to perform these calculations a cylindrical geometry version of the neutron kinetics, heat transfer code ZAPP has been written and tested against the experimental data from the SPERT III-E oxide core. The results of this comparison are given as an appendix to this report.

National Library of Australia card number and ISBN 0 642 59644 1

The following descriptors have been selected from the INIS Thesaurus to describe the subject content of this report for information retrieval purposes. For further details please refer to IAEA-INIS-12 (INIS: Manual for Indexing) and IAEA-INIS-13 (INIS: Thesaurus) published in Vienna by the International Atomic Energy Agency.

REACTOR CORES; TRANSIENTS; HIFAR REACTOR; COOLANTS; FLUID FLOW; REACTIVITY
INSERTIONS; REACTOR CORE DISRUPTION; CRITICALITY

CONTENTS

	Page
1. INTRODUCTION	1
2. CALCULATION OF HIFAR REACTIVITY COEFFICIENTS	1
3. SPERT II CORE BD22/24	2
4. THE HIFAR TRANSIENT MODEL	3
4.1 Boiling Heat Transfer and Void Development	4
5. RESULTS OF HIFAR CALCULATIONS - NO COOLANT FLOW	5
5.1 Discussion of Results - No Coolant Flow	5
5.2 Loss of Control Arm Blade	7
6. CALCULATIONS WITH COOLANT FLOW	7
6.1 Results of Calculations with Coolant Flow	7
7. CONCLUSIONS	8
Figure 1 Calculated (HIFAR) and measured (SPERT II core BD22/24) power burst parameters as a function of initial inverse period	9
Figure 2 Calculated components of the total reactivity compensation as a function of initial inverse period	10
Figure 3 Comparison of calculated burst shape parameters for HIFAR with observed values from SPERT II core BD22/24	11
Figure 4 Calculated power bursts for HIFAR under conditions of forced coolant flow	12
Appendix A Calculation of Power Transients in the SPERT III-E Oxide Core	13
Figure A1 Calculated and measured values of peak power as a function of initial inverse period for SPERT III-E core	17
Figure A2 Calculated and measured values of energy release as a function of initial inverse period for SPERT III-E core	18
REFERENCES	19

1. INTRODUCTION

In previous studies of the consequences of reactivity additions above critical, Corran and McCulloch [1968] and Wilson [1972] have considered the power transients to be terminated by the action of power level or period trips, although Turner [1965] prepared a qualitative estimate of steam void formation shutdown.

The present work is an examination of the power transient behaviour of the AAEC's research reactor HIFAR without consideration of the effects of actuation of the installed safety system. Reactivity feedback coefficients were obtained by four-group, two-dimensional diffusion theory calculations. The method of calculating power transients was that developed by Clancy *et al.* [1975, 1976] and Connolly and Harrington [1977] in analysing transient data from the SPERT program. Specific sequences of events leading to the initiation of a power transient are not examined, except for the case where a central coarse control arm blade is supposed to fall out from the core. However, the results presented should enable conclusions to be drawn as to the consequences of simple accident situations and whether further calculations are warranted.

Because of the annular geometry of the HIFAR fuel element, a one-dimensional cylindrical geometry version of the transient analysis code ZAPP had to be written (Clancy, AAEC report to be published). This version was tested against experimental data from the SPERT III-E oxide core; a comparison of calculated and measured transient parameters is given in Appendix A.

2. CALCULATION OF HIFAR REACTIVITY COEFFICIENTS

A fundamental difficulty with calculation of real and adjoint flux distributions in HIFAR is the large difference between the minimum 'cold clean' critical mass of approximately 1 kg ^{235}U and the fuel loading for normal operation of approximately 3.2 kg ^{235}U . A rigorous calculation should therefore include the spatial distribution of neutron absorption by the coarse control arm bank and the rigs present in experimental facilities.

Since this is a formidable problem, an XY model of the reactor was set up and criticality forced by two methods; the first (method A) by a criticality search on the core axial buckling B_z^2 and the second (method B) by a uniform poisoning of the core and reflector. The intention was to demonstrate the sensitivity of perturbation calculations to the real and adjoint fluxes obtained by the two methods. Results obtained are shown in Table 1.

Use of the mean values of Table 1 in calculating the whole reactor temperature coefficient at 45°C gives the value of $-4.1 \times 10^{-4} \text{ }^\circ\text{C}^{-1}$ which is in

TABLE 1
RESULTS OF HIFAR PERTURBATION CALCULATIONS

Perturbation	Reactivity Change $\delta k/k$		
	Method A	Method B	Mean (A,B)
1% density change in coolant	-1.59×10^{-3}	-0.92×10^{-3}	-1.26×10^{-3}
1 K change in coolant temperature	-2.18×10^{-4}	-2.94×10^{-4}	-2.56×10^{-4}
1% density change in all D ₂ O	-2.65×10^{-3}	-3.53×10^{-3}	-3.09×10^{-4}
1 K change in temperature of all D ₂ O	-2.58×10^{-4}	-3.03×10^{-4}	-2.8×10^{-4}

good agreement with the experimental value of $-4.2 \times 10^{-4} \text{ } ^\circ\text{C}^{-1}$ reported by Wilson [1972]. The largest contribution to this coefficient is from the change in neutron spectrum with change in the coolant temperature, and, since methods A and B differ by 35% in calculating this effect, the uncertainty in the calculated whole reactor temperature coefficient is considerably greater than that indicated by the comparison with the measured value above.

As shown later, in the range of transients for which fuel element cladding melting temperatures are approached, the major shutdown mechanism is produced by steam voiding of the coolant channels. Experimental values of fuel element void coefficients are few, and mainly confined to measurement of the reactivity effect following complete voiding of the 50.8 mm diameter central thimble of the fuel element. It is highly likely that neutron streaming in this voided thimble contributes substantially to the measured reactivity change, an effect not included in the calculated void coefficient, or present in the small void fraction which is needed to terminate a power transient. Using the mean value from methods A and B for the reactivity change from a 1% reduction in coolant density in the central fuel element gives $-0.33 \times 10^{-5} \delta k/k \text{ cm}^{-3}$ for the void coefficient, compared with the value quoted by Wilson [1972] of $-0.46 \times 10^{-5} \delta k/k \text{ cm}^{-3}$.

Although not entirely satisfactory, the reactivity coefficients used in the transient analysis described below are those obtained from averaging the components obtained by calculational methods A and B. Much of this uncertainty could be resolved by a systematic measurement of the void coefficient throughout the HIFAR core.

3. SPERT II CORE BD22/24

Self-terminating power excursion tests have been performed within the

SPERT program with a reactor core (BD22/24) very similar to that of HIFAR. This similarity is shown in Table 2, where the BD22/24 data are taken from Grund [1963].

The major differences between BD22/24 and HIFAR which affect the transient behaviour of these reactors are found in the values of the prompt neutron lifetimes, the heat transfer areas and coolant volumes/fuel element. The last will primarily affect the value of the transient reactivity feedback coefficient; an attempt has been made to calculate this for BD22/24 but without success. The problem lies with the very large critical mass given for this core which could not be reproduced by calculation. Direct calculation of power transients in BD22/24 to verify the HIFAR model has not therefore been possible; however some qualitative features of transient test results for this core are discussed later.

TABLE 2
COMPARISON OF DATA BETWEEN HIFAR AND BD22/24

Parameter	BD22/24	HIFAR
Number of fuel elements	24	25
Lattice pitch (mm)	152.4	152.4
Fuel plate geometry	flat slab	annular
Fuel alloy thickness (mm)	0.508	0.432
Coolant channel thickness (mm)	1.85	3.40
²³⁵ U/fuel element (g)	154	150
Heat transfer area (m ²)	40	29
Prompt neutron lifetime (μs)	~ 650	~ 400
Max/average core power	1.5	1.6
Clean cold critical mass (kg)	2.8	~ 1.0
Coolant volume/fuel element (ℓ)	1.5	2.5
Whole reactor temperature coefficient (δk/k °C ⁻¹)	-3.3 x 10 ⁻⁴	-4.2 x 10 ⁻⁴
Central void coefficient (δk/k cm ⁻³)	-0.22 x 10 ⁻⁵	-0.46 x 10 ⁻⁵

4. THE HIFAR TRANSIENT MODEL

The annular geometry of the HIFAR fuel element requires that a cylindrical geometry option be written into the transient analysis code ZAPP. This option has been checked by comparing transients calculated by ZAPP for the SPERT III-E

oxide core with experimental data. The results are given in Appendix A.

The complexity of the HIFAR fuel element and the relative uncertainty in the spatial distribution of the reactivity feedback coefficient in the core have led to some simplifications:

- reactivity feedback from metal expansion has been neglected;
- reactivity feedback coefficients have not been weighted by a power distribution;
- flux fine structure within the fuel element has been neglected and the reactivity feedback coefficients have been allocated to the coolant channels on the basis of the fractional volume of coolant within each channel;
- the mesh structure was made coarser to accomplish a reasonable code running time and to meet restrictions on the permitted number of regions. (Even so, the fuel element was represented by 94 regions and 182 mesh points); and
- only fission energy appearing directly in the fuel alloy (95%) was listed in the input. (Indirect heating from neutron slowing down and gamma ray absorption was neglected because of the likelihood that most of this heat would appear outside the fuel element.)

All these approximations are believed to be either conservative or of minor influence on the calculated transient behaviour.

4.1 Boiling Heat Transfer and Void Development

Boiling heat transfer shutdown was assumed to commence in the core when the central fuel element cladding reaches 100°C. Steam void formation was assumed to commence when the temperature at the same location reaches 150°C and to grow at the linear rate of 250 μ s⁻¹ thus generating reactivity feedback at the rate of -0.5 $\delta k/k$ s⁻¹. As it will be shown that steam void formation as a shutdown mechanism becomes important in HIFAR at much lower values of initial inverse asymptotic period (α_0) than in the SPERT I cores, this simple model of steam void growth will be discussed in more detail.

Clancy *et al.* [1976] found that the void development rate of 250 μ s⁻¹ commencing at a central core cladding of 150°C provided a good fit to transient data measured on SPERT I core D12/25. For this core, a central temperature of 150°C implies that \sim 70% of the core heat transfer area has a temperature in the range of 100 - 150°C. If boiling steam voids are assumed to develop uniformly over this area, then the total rate of void development of 250 μ s⁻¹ corresponds to a rate per unit heat transfer area of 16 mm s⁻¹.

Void volume development data, obtained by photographic observations on thin platinum ribbons immersed in water and exponentially heated, have been reported by Johnson *et al.* [1961]. If the early stage of void development and collapse, caused by the very low heat capacities of these ribbons, is ignored, and a straight line fitted to the remainder of the data, rates of void development per unit area of between 10 and 26 mm s⁻¹ are obtained for values of initial inverse period in the range from 70 s⁻¹ to 200 s⁻¹. It is over a similar range of α_0 (40 s⁻¹ - 300 s⁻¹) that a void growth rate/unit area of 16 mm s⁻¹ was found to provide a good fit to D12/25 transient data.

However, the limited data of Johnson *et al.* indicate that for smaller values of α_0 the rate of void formation decreases rapidly, three values for $10 \text{ s}^{-1} < \alpha_0 < 40 \text{ s}^{-1}$ being $\sim 1 \text{ mm s}^{-1}$. As will be shown, this is the range of α_0 for which void formation is important in terminating HIFAR transients if the assumption of a 'trigger' temperature of 150°C is correct. Use of the voiding rate derived from D12/25 in HIFAR calculations does, however, reproduce the burst shape parameter $\alpha_0 E_{tm}/P_{max}$ observed in the SPERT II core BD22/24 and so it has been retained in the calculations reported here.

5. RESULTS OF HIFAR CALCULATIONS - NO COOLANT FLOW

Burst parameters for a range of step additions of reactivity above critical, producing asymptotic reactor periods in the range from one second to twenty-five milliseconds are shown in Figure 1, where the following symbolism has been used:

- P_{max} - peak reactor power (MW)
- E_{tm} - energy release up to the time of peak power (MJ)
- θ_{tm} - maximum cladding temperature rise at the time of peak power (°C)
- t_{tm} - time to peak power (s)
- E_{tot} - total energy release in initial power pulse (MJ)
- θ_{max} - maximum cladding temperature rise produced during initial power pulse (°C).

Figure 2 shows reactivity insertion, total reactivity compensation and the components of the total reactivity compensation as a function of the initial inverse reactor period α_0 . Figure 3 shows the burst shape parameter $\alpha_0 E_{tm}/P_{max}$ as a function of α_0 .

5.1 Discussion of Results - No Coolant Flow

Figure 2 shows that for $\alpha_0 > 10 \text{ s}^{-1}$, the importance of steam formation to reactor shutdown increases rapidly; it equals the reactivity compensation from heating of the coolant for a transient characterised by $\alpha_0 = 14 \text{ s}^{-1}$, and is a factor of 2.5 larger for a transient in which $\alpha_0 = 40 \text{ s}^{-1}$. Thus, in the

range of α_0 where core damage may be expected, the steam shutdown model plays the dominant role in the calculated power history.

As a check on the validity of the steam formation model used in these calculations, the computed shape factor $\alpha_0 E_{tm}/P_{max}$ for HIFAR is compared with the experimental results from the SPERT II BD22/24 core in Figure 3. Grund [1963] quotes a value of $0.25 \times 10^{-5} \delta k/k \text{ cm}^{-3}$ for the central void coefficient in BD22/25 which may be compared with the mean computed value of $0.32 \times 10^{-5} \delta k/k \text{ cm}^{-3}$ for HIFAR. This similarity, together with the similar ratios of maximum/average reactor power, makes it plausible to expect that the steam void induced reactivity effects will be similar in the two reactors; Figure 3 shows excellent agreement between the calculated shape factors for HIFAR and those measured in BD22/24. This shape factor, a measure of the rapidity with which the power rise is arrested, has the value 2.0 in the prompt critical region for a shutdown in which the reactivity feedback remains proportional to energy release, and the value 1.0, for an exponential sawtooth shaped power pulse. The value of 1.25 observed in both experiment and calculation demonstrates the markedly non-linear shutdown effects operating in these transients.

Figure 1 shows that for a transient in which $\alpha_0 = 40 \text{ s}^{-1}$ the maximum cladding temperature is 380°C , peak power 330 MW and the total energy release 23 MJ. At the time of peak power, 5.75 ℓ of steam void has been produced (volume of coolant in one element 2.5 ℓ) and, at the conclusion of the initial power burst when the reactor power has fallen below, say, 10 MW, 23 ℓ of steam. Clearly in an excursion of this magnitude, occasioned by the injection of 2.4% $\delta k/k$ into a just-critical core at low power, a substantial number of fuel elements will be more or less completely voided. This result is in agreement with the conclusions of Grund [1963], who inferred that step reactivity addition of 2.6% $\delta k/k$ is enough to cause localised melting of fuel plates in core BD22/24.

Also shown in Figure 1 are the energy release and temperature data reported for core BD22/24. Note that, although E_{tm} values are more than twice those of HIFAR, the temperature data are in much closer agreement. If the reactivity feedback coefficients of the two reactors were similar, this result would be expected because the most important parameters would then be the heat transfer areas and prompt neutron lifetimes of the two cores. Table 1 shows that the ratios of these quantities for BD22/24 and HIFAR are 1.38 for the heat transfer area and 1.62 for the prompt lifetime, giving an expected factor of 2.24 between the energy releases for the two reactors at the same value of α_0 .

5.2 Loss of Control Arm Blade

The method usually postulated for the accidental addition of a large reactivity step in HIFAR is for a control arm blade to break and fall out of the core. Assuming, after Corran and McCulloch [1968], that a central control arm is involved, and its reactivity worth is 26% of the total bank worth, it may be deduced from the present work that if the reactivity controlled by the control arm bank at the time of the central arm break was 9.2% $\delta k/k$, then the core would suffer local meltdown during the initial power pulse.

Figure 1 shows that the proportionality of t_{tm} to α_0^{-1} implies that most of the reactivity feedback occurs close to the time of peak power. (Since these calculations assume an initial reactor power of 10 kW, values of t_{tm} for other values of initial power P_0 (watts) may be obtained by adding a time $1/\alpha_0 \ln(10^4/P_0)$ to the values of t_{tm} given in Figure 1.) Thus for all except the fastest transients shown in Figure 1, there is a considerable time interval for installed shutdown mechanisms to determine the course of a transient, if such mechanisms are actuated by period trips. By way of example, a transient for which the initial period is 50 ms, initiated at a power level of 500 watts, would require a time of 500 + 150 ms to reach a peak power determined by the reactivity feedback coefficients of the reactor. This time is sufficiently long to enable the control arm scram to play a decisive part in terminating the transient.

Further analysis of the efficacy of the installed shutdown mechanisms requires that a detailed sequence of accident events and initial core conditions be postulated. Provided the additional shutdown mechanisms can be reasonably represented as a linear ramp of reactivity, ZAPP is capable of calculating the consequences of such accidents.

6. CALCULATIONS WITH COOLANT FLOW

The necessity of providing axial sub-division in the reactor core for the ZAPP flow model [Connolly & Harrington 1977] prohibited the use of the explicit geometry fuel element model of the preceding sections because of the limitations of the number of zones/regions in the ZAPP code. Instead, the semi-infinite slab cell approximation was used, and comparison of this model with no coolant flow with the zero coolant flow cylindrical model showed that the calculated transient parameters were some 35% lower in the former case. To this extent the results given for power transients under conditions of coolant flow are uncertain.

6.1 Results of Calculations with Coolant Flow

Figure 4 shows the power histories of the reactor following a represent-

ative range of step reactivity inputs. Discussion of these results is difficult because of the complex interaction of flow, boiling heat transfer and reactivity feedback. However, it may be noted that for initial reactor periods less than the transit time of the coolant across the core (156 ms), the first power peak is similar in magnitude to that obtained in the no-flow case; the major effect of flow is seen in the post peak power variation. For periods much longer, the sharply defined power peak disappears and the reactor power rises to a quasi-equilibrium level much greater than the peak power obtained for the same period under no-flow conditions.

7. CONCLUSIONS

Power transients under no-coolant flow conditions have been calculated for HIFAR for a range of step reactivity additions to the core. Because a realistic model of the HIFAR fuel element has been used, it is considered that the principal uncertainty in these calculations is the magnitude of the reactivity feedback coefficient and the steam void rate of negative reactivity insertion. The close similarity between the calculated burst shape parameters for HIFAR and BD22/24, gives confidence that the errors for HIFAR are not large. Therefore the estimate of 2.4% $\delta k/k$ as the reactivity step required to produce significant core damage is considered reliable.

The uncertainties in the case of the calculated transients with coolant flow through the core are much greater, because of both the simple representation of the fuel element, and the fact that the flow model itself has been tested against only a relatively small range of experimental data. However, in the range of transients for which core damage might be expected, the transit time of the coolant through the core is sufficiently long, compared with the reactor periods, to ensure that the effects of coolant flow are significant only in the post-peak time interval.

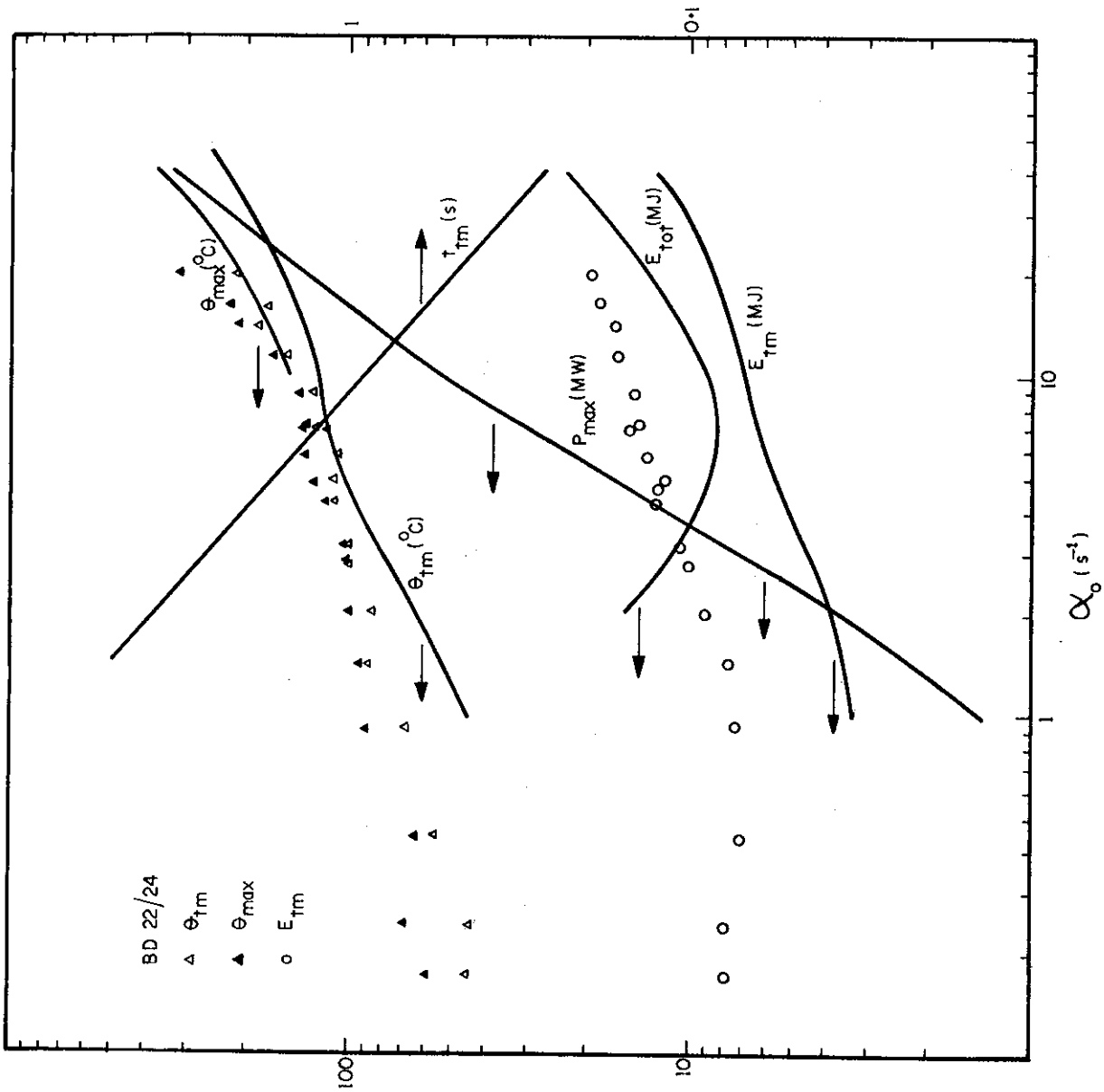


FIGURE 1. CALCULATED (HIFAR) AND MEASURED (SPERT II CORE BD22/24) POWER BURST PARAMETERS AS A FUNCTION OF INITIAL INVERSE PERIOD

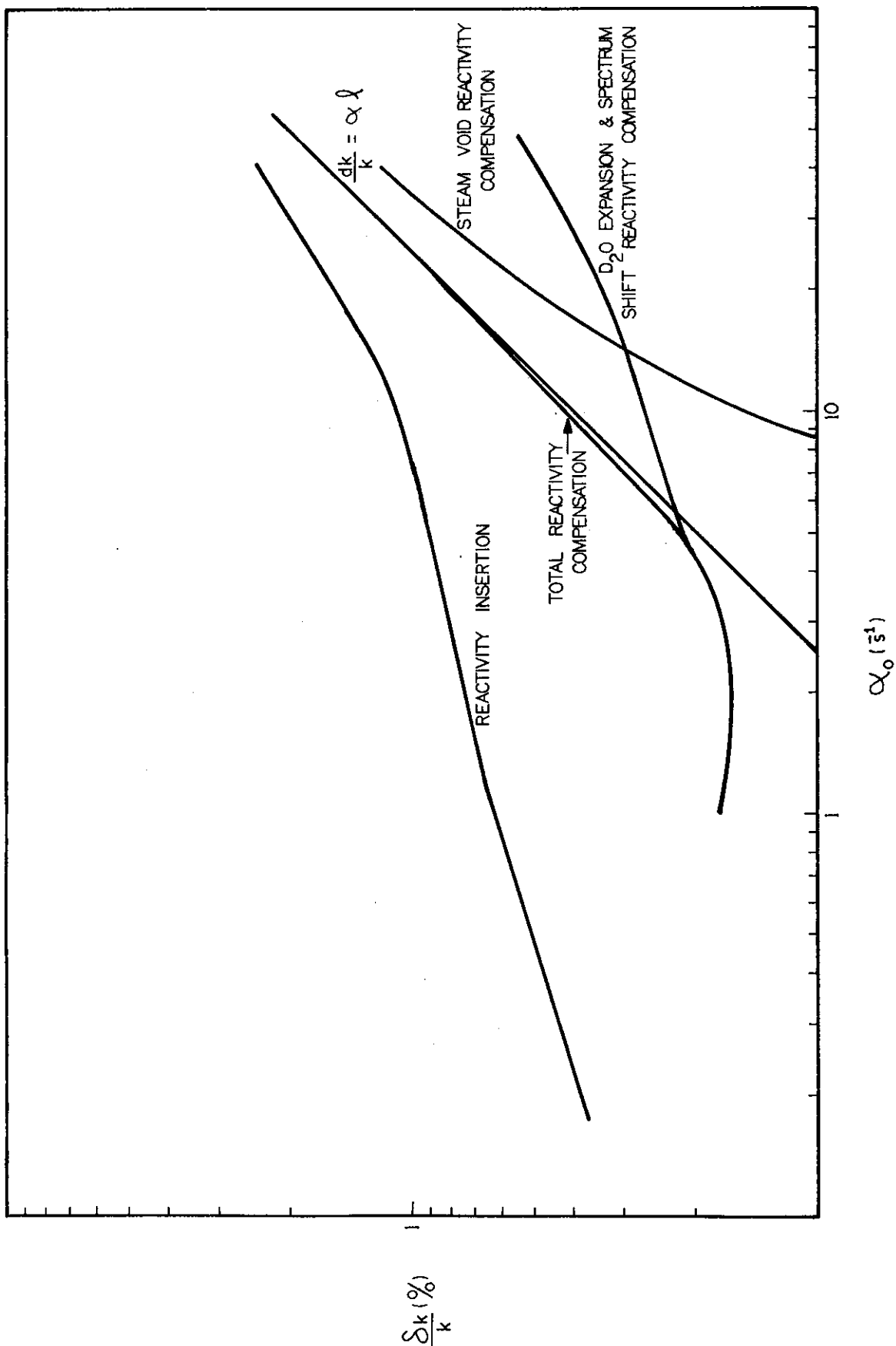


FIGURE 2. CALCULATED COMPONENTS OF THE TOTAL REACTIVITY COMPENSATION AS A FUNCTION OF INITIAL INVERSE PERIOD

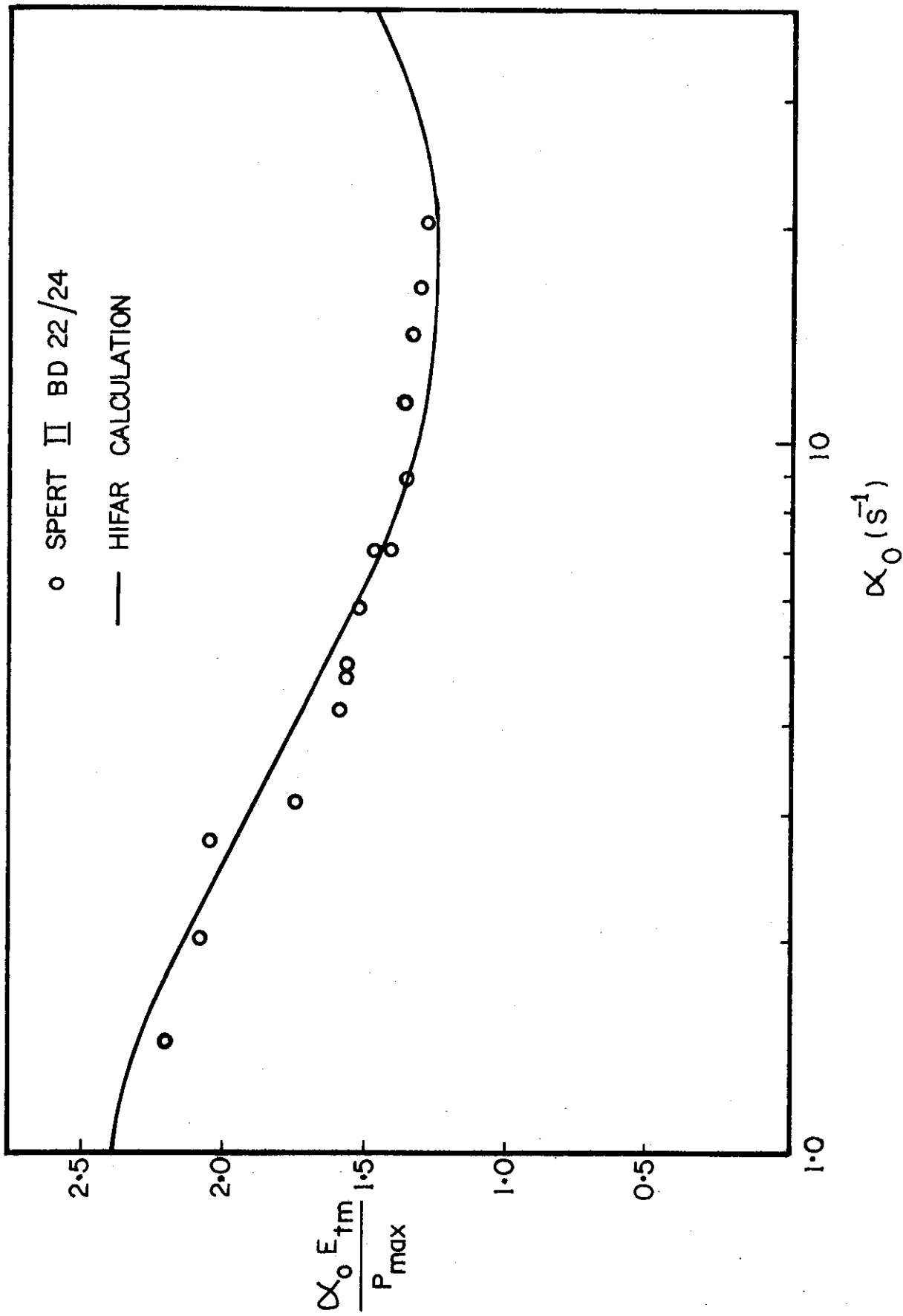


FIGURE 3. COMPARISON OF CALCULATED BURST SHAPE PARAMETERS FOR HIFAR WITH OBSERVED VALUES FROM SPERT II CORE BD22/24

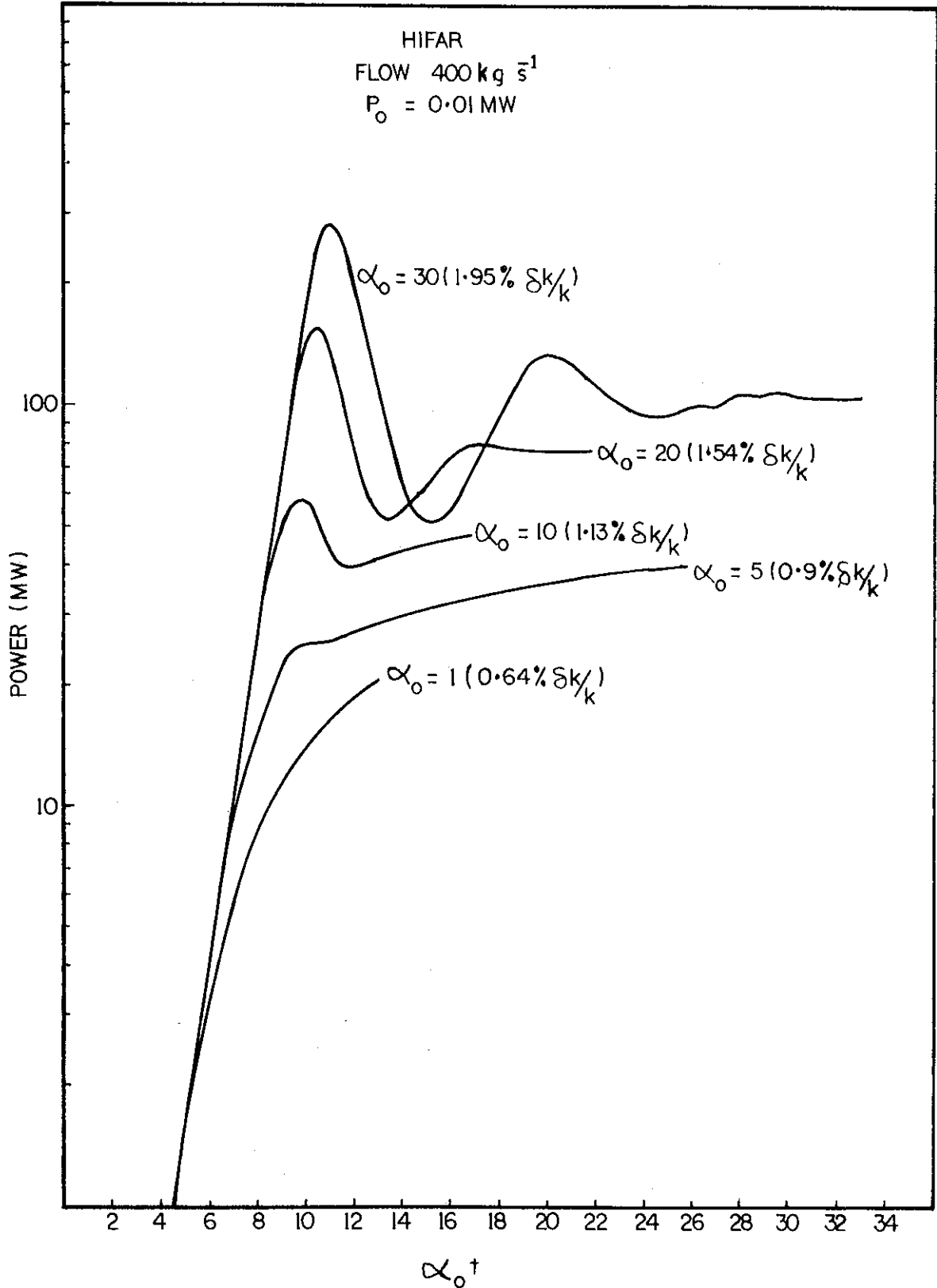


FIGURE 4. CALCULATED POWER BURSTS FOR HIFAR UNDER CONDITIONS OF FORCED COOLANT FLOW

APPENDIX ACALCULATION OF POWER TRANSIENTS IN THE SPERT III-E OXIDE CORE

The SPERT III-E oxide core was a small mock-up of a typical PWR core. Power transient data were obtained for a range of initial core conditions corresponding to those encountered in operation of a commercial unit. A description of this reactor and the experimental results have been given by McCardell *et al.* [1965].

Calculations of power transients in this core have been made to test the cylindrical cell option of ZAPP and to further test the coolant flow model used in the analysis of SPERT II transients by Connolly and Harrington [1977].

The SPERT III-E core fuel pin consisted of a UO₂ pellet, radius 5.334 mm a helium gas gap of 0.076 mm and stainless steel cladding, thickness 0.508 mm. These pins were mounted in the fuel elements in a 5 x 5 array on a square lattice pitch of 14.86 mm. The coolant area was converted into an annular region of the same area for the ZAPP cell representation. The value of the gas gap thermal conductivity was taken from data given by McCardell *et al.* [1965], as were values of the fuel Doppler coefficient and coolant void coefficient. The coolant spectrum reactivity coefficient was inferred from the data of McCardell *et al.* by assuming a reflector spectrum reactivity coefficient of $10^{-4} \delta k/k \text{ } ^\circ\text{C}^{-1}$, [Wajima and Yamamoto 1965].

The system conditions for the E core experiments were as follows:

<u>Accident Conditions</u>	<u>Coolant Inlet Temperature</u>	<u>Initial Reactor Power</u>
Cold start-up	21°C	5×10^{-5} MW
Hot start-up	127°C or 260°C	5×10^{-5} MW
Hot standby	260°C	1 MW
Operating power	260°C	20 MW

ZAPP Calculations of cold start-up transients are shown in Figures A1 and A2. Excellent agreement with experiment is shown over the whole range of experiment.

A comparison of calculated and measured burst parameters for a representative range of hot start-up excursions is given in Table A1. Good agreement between experiment and calculation is demonstrated.

Only a limited number of hot standby and operating power transients were measured in the experimental program, and all tests were for a coolant flow rate of 427 ms^{-1} . Table A2 shows the results of experiment and calculation. In the case of operating power transients, it was found that the calculations

APPENDIX A (continued)

TABLE A1
HOT STARTUP EXCURSIONS

α_0 (s ⁻¹)	Flow (ms ⁻¹)	P _{max} (MW) C	P _{max} (MW) E	C/E	E _{tm} (MJ) C	E _{tm} (MJ) E	C/E
Initial Temperature 120°C: Pressure 10 MPa							
97.1	4.27	295	280±42	1.05±0.15	6.25	6.3±1.1	0.99±0.17
51.0	4.27	86.7	78±12	1.11±0.15	3.50	3.2±0.5	1.09±0.16
23.5	4.27	23.7	22±3	1.08±0.14	2.29	2.0±0.3	1.14±0.15
9.8	4.27	10.7	9.1±1.4	1.17±0.15	4.27	4.3±0.7	0.99±0.16
4.78	4.27	7.8	6.8±1.0	1.15±0.15	~9.5*	7.6±1.3	-
14.31	6.70	13.6	11±2	1.24±0.18	2.77	3.2±0.5	0.86±0.16
8.48	7.3	9.6	7.8±1.2	1.23±0.15	5.39	4.8±0.8	1.12±0.17
Initial Temperature 260°C: Pressure 10 MPa							
103	4.27	475	410±41	1.16±0.10	9.13	8.5±1.1	1.07±0.13
48.5	4.27	115	97±10	1.18±0.11	4.77	4.5±0.6	1.06±0.13
14.24	4.27	19.8	16±2	1.24±0.12	4.44*	3.3±0.4	-

*Broad topped bursts - E_{tm} not well defined

were very sensitive to the rate at which the excess reactivity was inserted. This is because the initial power level was so high that reactivity feedback commenced while the reactivity was being inserted and the reactor did not attain an asymptotic period. The rate of reactivity insertion was estimated from rod withdrawal rates given by McCardell *et al.* [1965] as 0.121 s⁻¹; the effect of increasing this to 0.125 s⁻¹ is also given in Table A2.

Again, satisfactory agreement between experiment and calculation is obtained, although to make the comparison meaningful, the operating power test would require very precise knowledge of the reactivity insertion rate. Examination of the reactivity compensation data shows that the major part comes from the Doppler effect in the fuel and this fact, together with the low thermal conductivity of the oxide fuel, makes these transients more insensitive to flow rate than the highly enriched, thin fuel plates of the SPERT II reactor.

APPENDIX A (continued)

TABLE 2A

HOT STANDBY AND OPERATING POWER EXCURSIONS

Reactivity Insertion ($\delta k/k$)	Conditions	P_{\max} (MW) C	P_{\max} (MW) E	C/E	E_{tm} (MJ) C	E_{tm} (MJ) E	C/E
0.00959	Hot	141	120±10	1.18±0.08	4.9	4.5±0.6	1.09±0.13
0.0108	Standby	704	620±60	1.13±0.10	11.3	11±1	1.03±0.09
0.121 s ⁻¹	Operating	439	610±60	0.72±0.10	11	17±2	0.64±0.12
0.125 s ⁻¹		590	610±60	0.97±0.10	13	17±2	0.76±0.12

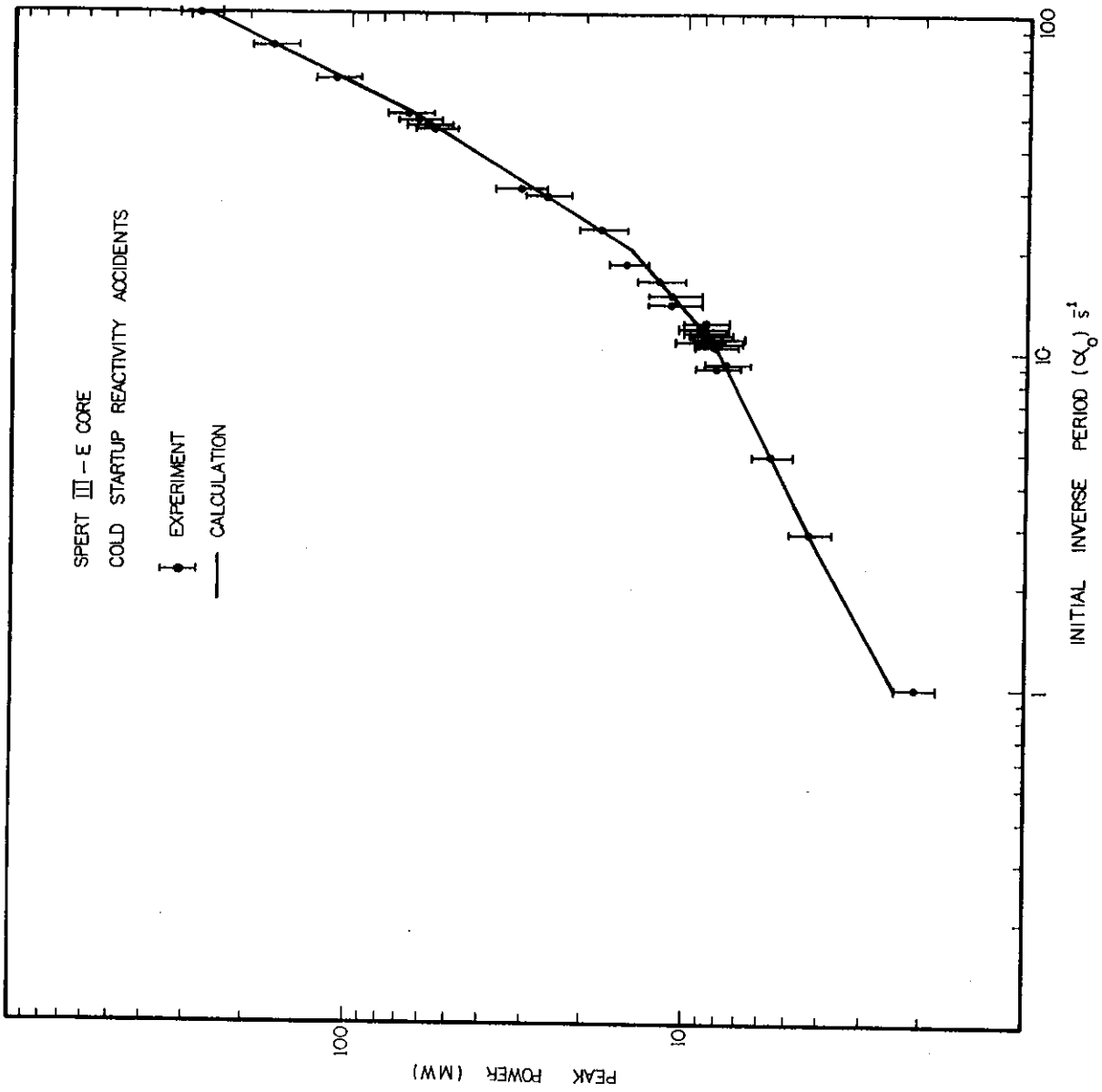


FIGURE A1. CALCULATED AND MEASURED VALUES OF PEAK POWER AS A FUNCTION OF INITIAL INVERSE PERIOD FOR SPERT III-E CORE.

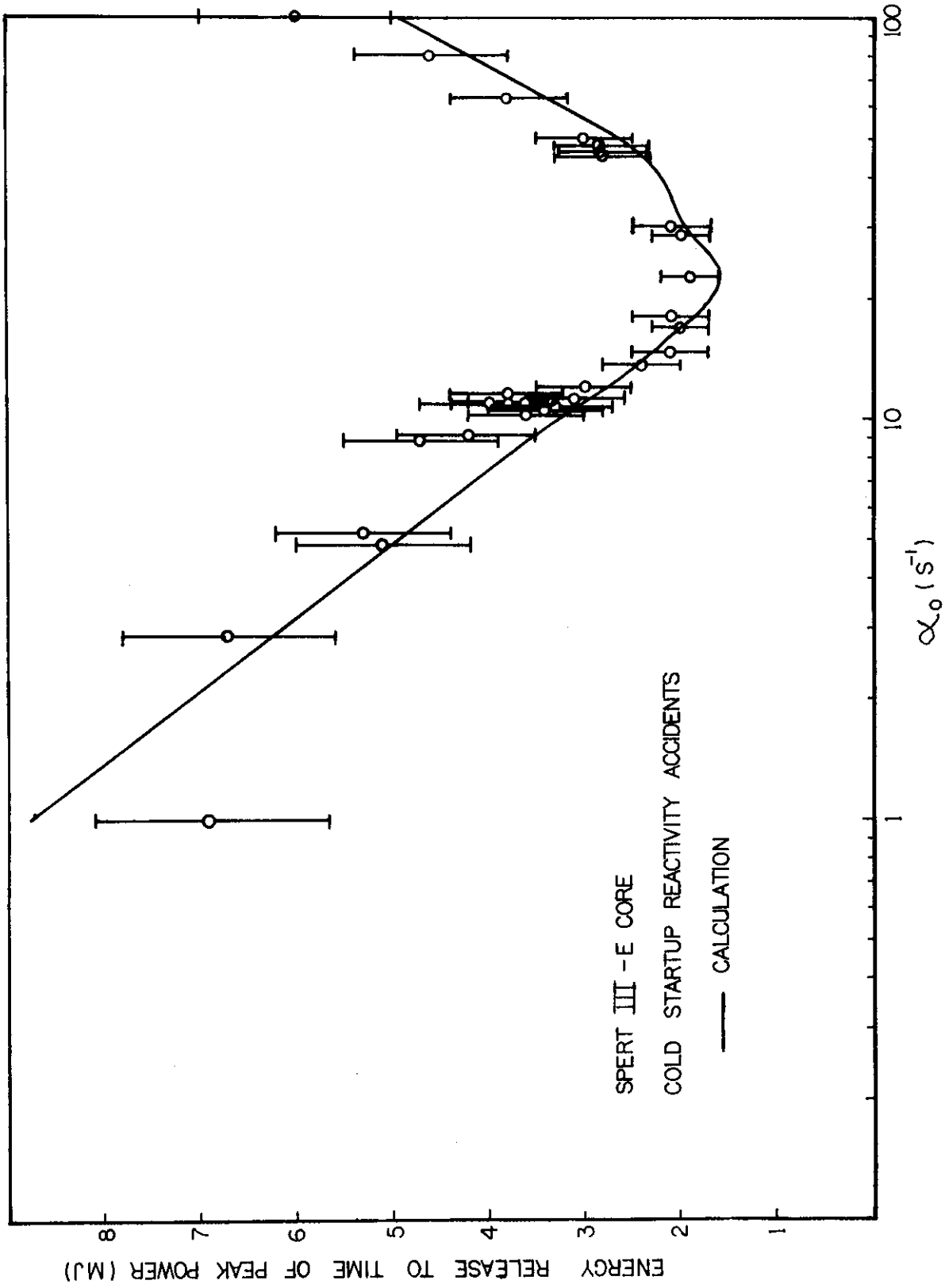


FIGURE A2. CALCULATED AND MEASURED VALUES OF ENERGY RELEASE AS A FUNCTION OF INITIAL INVERSE PERIOD FOR SPERT III—E CORE.

REFERENCES

- Clancy, B.E., Connolly, J.W. & Harrington, B.V. [1975] - An analysis of power transients observed in SPERT I reactors. Part I, AAEC/E345.
Part II [1976] AAEC/E383.
- Connolly, J.W. & Harrington, B.V. [1978] - AAEC/E report (to be published).
- Corran, E.R. & McCulloch, D.B. [1968] - Analogue studies of power transients following loss of a single coarse control arm blade in the materials testing (DIDO-type) reactor HIFAR. AAEC/TM479.
- Grund, J.E. [1963] - Self limiting excursion tests of a highly enriched plate type D₂O-moderated reactor. Part I. Initial Test Series IDO 16891.
- Johnson, H.A., Schrock, V.E., Selph, F.B., Lienhard, J.H. & Rosztoczy, Z.R. [1961] - Temperature variation, heat transfer and void volume development in the transient atmospheric boiling of water. SAN 1001.
- McCardell, R.K., Herborn, D.I. & Houghtailing, J.E. [1965] - Reactivity accident test results and analyses for the SPERT III-E core - a small oxide fuelled, pressurised water reactor. IDO 17281.
- Turner, W.J. [1965] - AAEC internal report.
- Wajima, J.T. & Hamamoto, K. [1965] - Temperature coefficient of water lattices. J. Nucl. Sci. and Tech. 2, 9, 331-339.
- Wilson, D.J. [1972] - AAEC internal report.

